Fraunhofer Institut
Techno- und
Wirtschaftsmathematik

A. Zemitis

On interaction of a liquid film with an obstacle

Berichte des Fraunhofer ITWM, Nr. 27 (2001)

ISSN 1434-9973

Bericht 27 (2001)

Die Veröffentlichungen in der Berichtsreihe des Fraunhofer ITWM können bezogen werden über:

Fraunhofer-Institut für Techno- und
Wirtschaftsmathematik ITWM
Gottlieb-Daimler-Straße, Geb. 49

67663 Kaiserslautern

Telefon: +49 (0) 6 31/2 05-32 42
Telefax: +49 (0) 6 31/2 05-41 39
E-Mail: info@itwm.fhg.de
Internet: www.itwm.fhg.de

Vorwort

Das Tätigkeitsfeld des Fraunhofer Instituts für Techno- und Wirtschaftsmathematik ITWM umfasst anwendungsnahe Grundlagenforschung, angewandte Forschung sowie Beratung und kundenspezifische Lösungen auf allen Gebieten, die für Techno- und Wirtschaftsmathematik bedeutsam sind.

In der Reihe »Berichte des Fraunhofer ITWM« soll die Arbeit des Instituts kontinuierlich einer interessierten Öffentlichkeit in Industrie, Wirtschaft und Wissenschaft vorgestellt werden. Durch die enge Verzahnung mit dem Fachbereich Mathematik der Universität Kaiserslautern sowie durch zahlreiche Kooperationen mit internationalen Institutionen und Hochschulen in den Bereichen Ausbildung und Forschung ist ein großes Potenzial für Forschungsberichte vorhanden. In die Berichtreihe sollen sowohl hervorragende Diplom- und Projektarbeiten und Dissertationen als auch Forschungsberichte der Institutsmitarbeiter und Institutsgäste zu aktuellen Fragen der Techno- und Wirtschaftsmathematik aufgenommen werden.

Darüberhinaus bietet die Reihe ein Forum für die Berichterstattung über die zahlreichen Kooperationsprojekte des Instituts mit Partnern aus Industrie und Wirtschaft.

Berichterstattung heißt hier Dokumentation darüber, wie aktuelle Ergebnisse aus mathematischer Forschungs- und Entwicklungsarbeit in industrielle Anwendungen und Softwareprodukte transferiert werden, und wie umgekehrt Probleme der Praxis neue interessante mathematische Fragestellungen generieren.

Prof. Dr. Dieter Prätzel-Wolters
Institutsleiter

Kaiserslautern, im Juni 2001

On interaction of a liquid film with an obstacle

A. Zemitis

August 6, 2001

Abstract

In this paper mathematical models for liquid films generated by impinging jets are discussed. Attention is stressed to the interaction of the liquid film with some obstacle. S. G. Taylor [Proc. R. Soc. London Ser. A 253, 313 (1959)] found that the liquid film generated by impinging jets is very sensitive to properties of the wire which was used as an obstacle. The aim of this presentation is to propose a modification of the Taylor's model, which allows to simulate the film shape in cases, when the angle between jets is different from 180°. Numerical results obtained by discussed models give two different shapes of the liquid film similar as in Taylors experiments. These two shapes depend on the regime: either droplets are produced close to the obstacle or not. The difference between two regimes becomes larger if the angle between jets decreases. Existence of such two regimes can be very essential for some applications of impinging jets, if the generated liquid film can have a contact with obstacles.

Introduction

Recently impinging jets are used as impinging-jet injectors for droplet generation [1, 2, 3]. The main characteristics of the impinging jets, which are interesting for developers of corresponding devices, are the shape of the liquid film and the droplet distribution. Fundamentals of the liquid sheet formed during impinging of jets can be found in papers of Taylor[4, 5, 6, 7]. It was shown there that the liquid film has a cardioid form and this fact follows from the properties of the anti-symmetrical waves in the liquid sheet. A smart analysis of the wave instabilities in the liquid sheet was done by N. Dombrowski and W.R. Johns [8]. They investigated also the size of ligaments and drops created during such processes. More detailed literature overview about earlier investigations regarding sheet form and droplet distribution can be found in [3, 2, 9]. A framework for the simulation of the impinging jets was done by E.A. Ibrahim and A.J. Przekwas [3]. They proposed prediction models of the film form, droplet size and distribution. In [10] the methods from Dombrowski and Johns for fan-spray nozzles regarding to droplet

size are transferred to impinging jets. In [2] atomization characteristics of sheets formed by laminar and turbulent impinging jets are studied experimentally. They propose some semi-empirical model for the droplets. In [9] an experimental study of the film thickness for impinging jets are presented.

In the practice there exist devices, where a contact of the liquid sheet with some surfaces can not be avoided. Our investigations are dedicated exactly to such kind of devices. Taylor [6] did analysis about the interaction of a wire with the liquid sheet. Other authors mainly are working with the free liquid sheets. Taylors results about interaction of the liquid film with wires are very interesting. It can be supposed that these results contain very deep physical phenomena, which need to be investigated. These phenomena can have a significant influence on the functionality of real devices based on impinging jets. In the paper regimes are investigated, where assumptions about Taylors cardioidal waves are fulfilled.

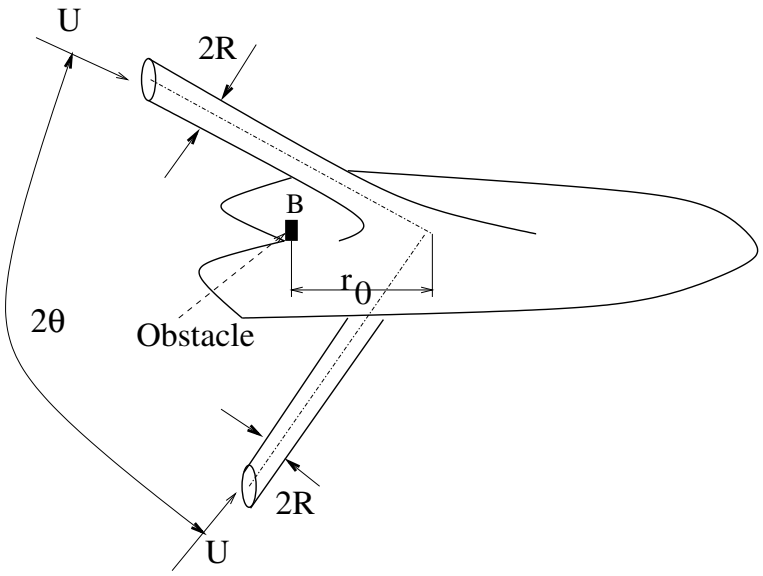

Figure 1: Interaction of the liquid film formed by impinging jets with an obstacle. Point B will also later show a position of the obstacle.

The principal scheme of the droplet generation process by impinging jets can be seen in Fig. 1. Two impinging jets with the radius R and with velocity U build a liquid film. On the film boundary droplets can be generated. In dependence of the angle between jets (2θ), different shapes of the film can be obtained.

Similar as in Taylor's paper [6], here will be investigated interaction a liquid film with some obstacle. In Fig. 1 the position of the obstacle is noted by point B. Taylor investigated interaction of the liquid film with a wire, if the angle $\theta = 90°$. The most important conclusion from his paper is that in experiments two different behaviors of the droplet generation can be observed. In one case

droplets are generated on the whole boundary of the liquid film starting from the obstacle. In the other case there exist a part of the boundary, where no droplets are produced. On this part the liquid is flowing in tangential direction along the boundary.

Our aim is:

- to simulate Taylor's experiments for the case $\theta = 90^\circ$ by using his mathematical models for the film shape,
- to propose a model and to do numerical experiments for the case $\theta \neq 90^\circ$.

Mathematical models for the film shape are some ordinary differential equations. Numerical solutions of these equations are obtained by the code "DDASSL" from Lawrence Livermore National Laboratory.

1 Models for film shape at $\Theta = 90^\circ$

As already indicated, Taylor analyzed in his paper [6] development of perturbation in the thin liquid sheets in the case when a vertical jet impacts on a flat impacter. The flow direction is perpendicular to the impacter and it corresponds to impinging jets, if the angle between jets is $2\theta = 180^\circ$. Such processes depend on Weber's number W_e [11]:

$$W_e = \frac{\rho_l U^2 R}{\sigma}, \tag{1}$$

where ρ_l, σ are density and surface tension of the liquid.

Taylor found that anti-symmetrical waves are responsible for spreading of the disturbances and that the velocity of these waves are independent of the wavelength (for low Weber's numbers, $We < 500$). A very important property is the following: if the sheet is moving with the velocity U, then the waves will be at rest in space if lines of constant phase are at the angle Ψ to the direction of flow, where:

$$sin\Psi = \left(\frac{2\sigma}{\rho_l h U^2}\right)^{0.5}, \tag{2}$$

and h is the thickness of the liquid sheet. Taylor rewrite the equation in other form:

$$sin^2\Psi = \frac{2\sigma}{\rho_l h U^2} = \frac{4\pi\sigma r}{\rho_l U Q} = \frac{r}{R_{max}}, \tag{3}$$

where Q is the volumetric flow rate per second and $R_{max} = \rho_l UQ/4\pi\sigma$. R_{max} is the limiting radius. No waves can remain at rest for $r > R_{max}$. The parameter R_{max} plays a similar role for water bells [4].

In polar co-ordinates (r, ϕ) the equation (2) can be integrated and so the presentation of the cardioid curves $r_e(\phi)$ can be obtained [5]:

$$r_e(\phi) = \frac{R_{max}}{2}(1 - cos(\phi - \phi_0)), \tag{4}$$

where θ_0 is a constant, which represents the angular position of an arbitrary point from which the wave is starting.

On the other hand it is possible to formulate some other equation for the film shape. Because the following relation is true [6]:

$$tan\Psi(\phi) = \frac{r_e(\phi)}{r'_e(\phi)}, \tag{5}$$

where $r'_e(\phi) = dr_e/d\phi$, then the equation (3) can be reformulated as follows:

$$\left(\frac{dr_e}{d\phi}\right)^2 = R_{max}r_e - r_e^2. \tag{6}$$

It is easy to test that the solution (4) fulfills the equation (6). If for some value of ϕ_0 the corresponding value $r_e(\phi_0) = r_0$ is given, then the shape of the liquid sheet can be estimated also by solving the equation (6). If the initial condition is $r_0 = R_{max}$ then for all ϕ: $r_e(\phi) = R_{max}$ (the circle corresponds to an undisturbed liquid film in the case $\phi = 90^\circ$).

Note, that one does not need to solve differential equation (6) for the simple case discussed above. However, reformulation of (3) in the form (6) is what allows us to treat more complex situations.

2 Taylors edge by $\theta = 90^\circ$

Taylor [6] has investigated interaction of the liquid film with some obstacle (a wire). The result was very sensitive to the properties of the wire (wet-ability, diameter). In some cases he observed experimentally that the properties of disturbed film can be different. There exist such perturbations, that on the one part of the film boundary droplets are not produced. The radial flow from the impact point changes on the film boundary direction, and the liquid flows there in the tangential direction. At the same time this fact has not a large influence on the other part of the film flow. As result there exists a point on the film boundary, where two types of boundary meet each other (from one side droplets are produced but from the other not). Mathematically this point corresponds to the switching point between different models and we will denote in Figures this point by the letter A. In Taylor's pictures of experiments point A can be observed as an edge on the film boundary. Close to this point the velocity vector has different directions.

Taylor [6] proposes also a mathematical model for the estimation of the film shape, if droplets are not produced. But he did not simulations with his model.

2.1 Model for the film without droplets

In this subsection the Taylor's model [6] is used. The model involves parameters which are defined on the film boundary and depend only on polar angle ϕ. Very essential is a scalar parameter q. The value qU characterizes the tangential speed of the liquid on the film boundary. Because in our case the obstacle has a position (r_0, π) and not $(r_0, 0)$ as in [6], Taylors equations can be rewritten as follows:

$$\frac{d}{d\phi}((\pi - \phi)q) = -cos\Psi, \tag{7}$$

$$1 - \frac{R_{max}}{r_e} sin^2\Psi = (\pi - \phi)q\frac{R_{max}}{r_e}\left(\frac{d\Psi}{d\phi} + 1\right) sin\Psi. \tag{8}$$

where again $(r_e(\phi), \phi)$ are polar coordinates of the film boundary, R_{max} were explained in connection to the formula (3). By using (5) a system of ordinary differential equations for $(r_e(\phi), q(\phi))$ can be obtained. It is convenient to have a system of first order equations. Therefore, an additional function $w = dr_e/d\phi$ is introduced, and a system for unknowns $(r_e(\phi), w(\phi), q(\phi))$ can be written:

$$\frac{dr_e}{d\phi} = w, \tag{9}$$

$$w^2 + r_e^2 - R_{max}r_e$$
$$= \frac{R_{max}}{r_e} q(\pi - \phi)\sqrt{\frac{r_e^2}{w^2 + r_e^2}}(2w^2 + r_e^2 - r_e\frac{dw}{d\phi}), \tag{10}$$

$$(\pi - \phi)\frac{dq}{d\phi} - q = -\sqrt{\frac{w^2}{w^2 + r_e^2}}. \tag{11}$$

The initial values are also proposed by Taylor [6], and in our case it means:

$$r_e(\pi) = r_0, \tag{12}$$

$$w(\pi) = -r_0\sqrt{\frac{R_{max} - r_0}{r_0}}, \tag{13}$$

$$q(\pi) = \sqrt{\frac{R_{max} - r_0}{R_{max}}}. \tag{14}$$

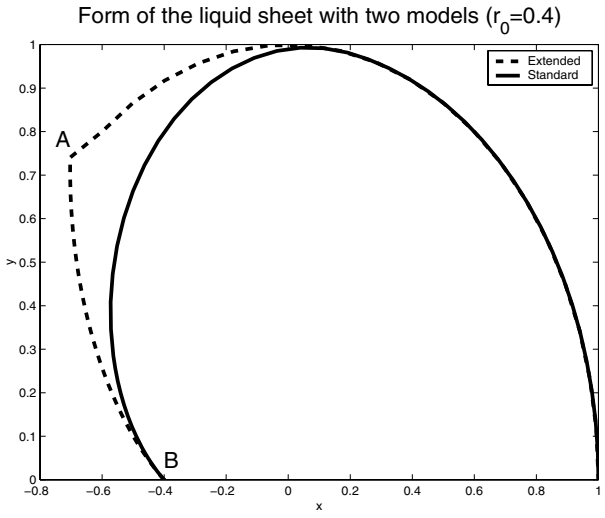

Figure 2: Simulation results corresponding to Taylors experiments, if droplets are produced on the whole edge (solid line) or only on one part (dotted line between B and A shows the part where droplets are not produced)

The problem (9)-(14) can be solved numerically for decreasing values of $\phi \leq \pi$ till some value $\phi = \phi_A$ (which corresponds to the point A). At this point $r_e(\phi_A) = R_{max}$. If the polar coordinate of the edge r_e reaches R_{max}, then droplets are produced and remaining part of the film has a constant polar coordinate $r_e = R_{max}$ for $\phi \in (\phi_A, 0)$. In the model the parameter R_{max} contains all flow parameters and the solution depends on the non-dimensional parameter $\frac{r_0}{R_{max}}$. Therefore, it can be assumed that $R_{max} = 1$ and the values of r_0 can be varied.

2.2 Model for the film with droplets

In the case if droplets are generated from the beginning (starting from the obstacle), then the model is based on the equation (6). For one half of the symmetrical shape the problem can be obtained:

$$\frac{dr_e}{d\phi} = -\sqrt{R_{max} r_e - r_e^2}, \phi < \pi \tag{15}$$

$$r_e(\pi) = r_0. \tag{16}$$

As it was mentioned, the solution of this problem can be written by using (4), but the problem can be solved also numerically.

2.3 Results

In Fig. 2 results of simulations obtained by two models are presented. Assume that: $R_{max} = 1$ and $r_0 = 0.4$. The solid line corresponds to the model (15)-(16) and is referred as standard solution. Here only one half of the symmetric solution is shown.

The standard solution shows the shape of the liquid film if the droplets are produced on the whole boundary.

The dotted line (noted as "extended" solution) corresponds to the model from subsection 2.1, when droplets are not produced near the obstacle. The part of the dotted line from the point B ($x = -0.4$) to the point A corresponds to the solution of the problem (9)-(14). The continuation of the line is described by $r_e = R_{max} = 1$. Here conditions for the droplet generation are fulfilled. This solution is similar to the Taylors experiment shown in Fig.III.6 [6]. As it was mentioned, Taylor observed experimentally two types of the liquid film in dependence of properties of the wire. In the paper [6] he wrote about the case if droplets are not produced: "It will be noticed also that the form of the edge is quite different from a cardioid which would have had greater curvature". The simulated curves have similar properties.

3 New model for $\theta \neq 90°$

In previous section described effect for liquid jets by $\theta = 90°$ is very interesting from the practical point of view. Small changes in the properties of obstacle can lead to qualitative changes in the behavior of the liquid film. Our aim is to investigate the following question: is it possibly to simulate a similar behavior for the liquid film in the case of inclined jets? For this purpose mathematical models are necessary, which can work also if an obstacle interacts with the liquid film.

For free liquid films in the case of inclined jets there exist a model, proposed by Ibrahim et. al. [3]. We will refer later to this model as to **model-I**. But by using model-I obstacles can not be directly accounted. Therefore, a modification of the model-I is done. By using of the modification it would be possible to estimate the film shape in the case, when on the whole film boundary droplets are generated.

For the regime, when droplets are not produced near the obstacle, the Taylor's model (7)-(8) has to be modified.

3.1 Modification of the model-I

The aim now is to obtain differential equation, which allows to construct the shape of the liquid film starting from any point close to the impact point. The main idea of modification (we will refer to this model as to model-IM) is that not

all assumptions of the model-I are used, but only one part of them. Nevertheless, the model-IM allows to estimate the film shape.

The model-IM includes several steps from model-I:

- Estimation of the parameter β, which depends on θ:

$$cos\theta = \left(\frac{e^{\beta}+1}{e^{\beta}-1}\right)\frac{1}{1+(\pi/\beta)^2}. \tag{17}$$

- Radius of the circle, where the initial thickness of the sheet is defined:

$$r_i = \frac{R}{sin\theta}. \tag{18}$$

- The initial thickness of the sheet $h_i(\phi,\theta)$ at the radius r_i:

$$h_i(\phi,\theta) = \beta R sin(\theta)/(e^{\beta}-1)e^{\beta(1-\phi/\pi)}. \tag{19}$$

- The thickness of the sheet $h(r,\phi,\theta)$ at any radial and angular position ϕ:

$$h(r,\phi,\theta) = h_i(\phi,\theta)\frac{r_i}{r}. \tag{20}$$

- Estimation of the thickness $h_e(\phi,\theta)$ of the edge can be done by using:

$$h_e(\phi,\theta) = \frac{2\sigma}{\rho_l U^2 sin^2\psi}. \tag{21}$$

and also by (20):

$$h_e(\phi,\theta) = h(r_e,\phi,\theta) = h_i(\phi,\theta)\frac{r_i}{r_e}, \tag{22}$$

where $r_e = r_e(\phi,\theta)$ describes the boundary of the liquid film.

This part of the model-I is sufficient for the estimation of the film shape. For inclined jets all characteristic parameters of the liquid film depend on θ. For shortening of terms this parameter will be omitted in the next expressions. From previous dependencies it can be obtained:

$$sin^2(\Psi(\phi)) = \frac{2\sigma(e^{\beta}-1)r_e(\phi)}{\rho_l U^2 \beta R^2 e^{\beta(1-\frac{\phi}{\pi})}}. \tag{23}$$

Similar as in (3) $\tilde{R}_{max} = \tilde{R}_{max}(\phi,\theta)$ can be introduced (we will omit θ):

$$\tilde{R}_{max}(\phi) = \frac{\rho_l U^2 \beta R^2 e^{\beta(1-\frac{\phi}{\pi})}}{2\sigma(e^{\beta}-1)}. \tag{24}$$

Now the equation (23) can be rewritten in the form

$$sin^2(\Psi(\phi)) = \frac{r_e(\phi)}{\tilde{R}_{max}(\phi)}. \tag{25}$$

Formally in (23) there are two unknowns $r_e(\phi)$ and $\Psi = \Psi(\phi)$. But because of formula (5) instead of (25) the following differential equation can be derived:

$$\frac{r_e^2(\phi)}{\left(\frac{dr_e(\phi)}{d\phi}\right)^2 + r_e^2(\phi)} = \frac{r_e(\phi)}{\tilde{R}_{max}(\phi)}. \tag{26}$$

Equation (26) is an ordinary differential equation with respect to the function $r_e(\phi)$. This function describes the shape of the liquid film, if droplets are produced on the film edge due to anti-symmetrical waves. This differential equation can be solved numerically, if an initial value for r_e is given. The model, which is based on the equation (26), we will refer to as to **model-IM**. Now it is possible to start calculation of the film from the position of the obstacle (point B). It is clear that the position of the obstacle must be not to far from the impact point: $r_0 \leq R_{max}(\phi)$.

3.2 Modified Taylors model for inclined jets

Taylor did his investigations about film edges, where no drops are produced in the case $\theta = 90°$. An interesting question is about such effect for inclined jets, but for solving of this problem the model (9)-(14) directly can not be applied. For Taylor it was important that the right hand side of the equation (III.6) does not depend on the angle ϕ. Now this is not true.

In Taylors investigation the parameter R_{max} is a constant. For inclined jets a new parameter $\tilde{R}_{max}$ dependent on ϕ and θ (24) is introduced. During of derivation of equations the steps from [6] are used as basis. Taylor takes as an important reference the value $r = R_{max}$. Now some other constant parameter must be used. If θ is fixed then r_i is a constant (see formula (18)). On the circle with radius r_i the initial thickness of the liquid sheet $h_i(\phi)$ (19) is defined. For the derivation of the model can be used the fact that the function $h_i(\phi, \theta)$ can be integrated in a simple way (we will omit θ):

$$\int h_i(\phi)d\phi = -\frac{\pi}{\beta}h_i(\phi) + C, \tag{27}$$

where C is some constant.

Assume that the position of the obstacle is (r_0, π), then the equation corresponding to Taylors equation (III.7) can be written as follows:

$$\frac{\pi}{\beta}(h_i(\phi) - h_i(\pi))\frac{dq}{d\phi} - h_i(\phi)q = -h_i(\phi)cos\Psi, \tag{28}$$

Instead of the Taylors equation (III.8) the following equation can be derived:

$$2\sigma - \rho_l U^2 h_e(\phi) sin^2\Psi = \frac{\rho_l r_i \pi U^2 q}{\beta}(h_i(\phi) - h_i(\pi))(\frac{d\Psi}{ds} + \frac{d\phi}{ds}). \quad (29)$$

By using $\tilde{R}_{max}(\phi)$ and the definition of the angle Ψ the system of equations can be formulated:

$$\frac{dr_e}{d\phi} = w, \phi < \pi, \quad (30)$$

$$\frac{\pi(\tilde{R}_{max}(\phi) - \tilde{R}_{max}(\pi))q}{\beta r_e}\sqrt{\frac{r_e^2}{r_e^2 + w^2}} \times(2w^2 + r_e^2 - r_e\frac{dw}{d\phi}) = w^2 + r_e^2 - \tilde{R}_{max} r_e, \phi < \pi, \quad (31)$$

$$\frac{\pi}{\beta}(h_i(\phi) - h_i(\pi))\frac{dq}{d\phi} - h_i(\phi)q = -h_i(\phi)\sqrt{\frac{w^2}{w^2 + r_e^2}}, \phi < \pi. \quad (32)$$

This is a system for three variables $(r_e(\phi), w(\phi), q(\phi))$. The initial values are estimated in a similar way as in [6].

$$r_e(\pi) = r_0, \quad (33)$$

$$w(\pi) = -r_0\sqrt{\frac{R_{max}(\pi) - r_0}{r_0}}, \quad (34)$$

$$q(\pi) = \sqrt{\frac{\tilde{R}_{max}(\pi) - r_0}{\tilde{R}_{max}(\pi)}}. \quad (35)$$

This model can be applied while

$$r_e(\phi) \leq \tilde{R}_{max}(\phi) \quad (36)$$

and it means that on the corresponding part of edge the droplets are not produced. In real simulations instead of the condition (36) some other condition is used. The switching to other model is done if $r_e(\phi) > 0.99\tilde{R}_{max}(\phi)$ (criterion for the switching point A).

Assume that the switching of models has to be done at $\phi = \phi_A$. Then for $\phi < \phi_A$ the model based on equation(26) must be used. The corresponding mathematical problem can be formulated as follows:

$$\frac{r_e(\phi)}{d\phi} = -\sqrt{\tilde{R}_{max}(\phi) r_e(\phi) - r_e^2(\phi)}, \phi_A > \phi > 0, \tag{37}$$

$$r_e(\phi_A) = 0.99 \tilde{R}_{max}(\phi_A). \tag{38}$$

The model describes the boundary of the liquid film where droplets are produced. To the complete model (30)-(38) we will refer as to **model-TI**.

4 Numerical experiments

The aim of numerical experiments is to investigate different regimes for droplet generation in the case of inclined jets. The main question is: can the model-TI really produce a solution which consists of two parts (existence of the similar edge A as in Fig. 2)? The other question is: how parameters of the liquid jets influence the position of the point A?

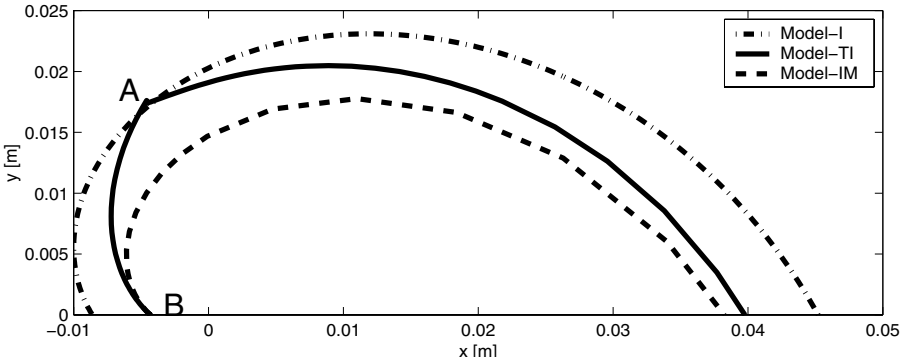

Figure 3: Simulation results with the model-TI, model-I and model-IM for inclined jets ($\theta = 70°$).

In simulations the following parameters are fixed: $U = 2.49m/s$, $\sigma = 0.073N/m$, $R = 0.75mm$. For the angle θ the values: $\theta = 70°$, $\theta = 60°$ and $\theta = 45°$ was chosen. The obstacle has the polar coordinate $r_e(\pi) = 0.5\tilde{R}_{max}(\pi, \theta)$.

The simulated results are shown in Fig. 3-5. Each figure contains 3 curves, obtained by model-I, model-TI and model-IM.

Model-I means that the curve is obtained purely by the model, proposed by Ibrahim et. al. [3]. In this case the obstacle is not taken into account and this curve corresponds to the free liquid film.

Model-IM is the discussed above modification of the model-I.

This allows to start the curve at every point where $r_e(\pi) < \tilde{R}_{max}(\pi, \theta)$. In this case droplets are produced on the whole boundary. The curve starts at the point $r_e(\pi) = 0.5\tilde{R}_{max}(\pi, \theta)$ because of obstacle.

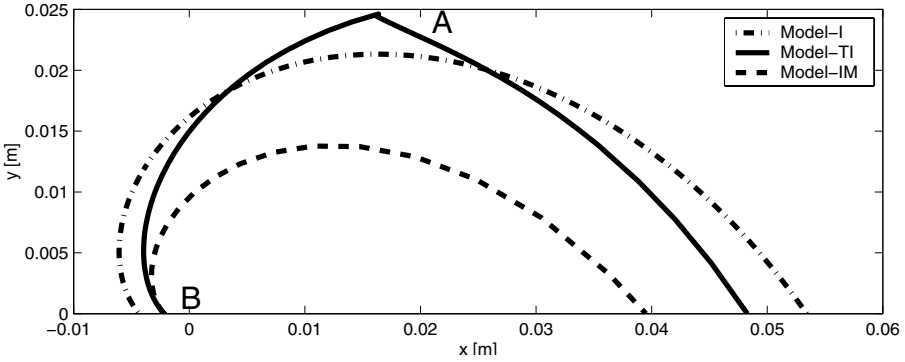

Figure 4: Simulation results with the model-TI, model-I and model-IM for inclined jets ($\theta = 60°$).

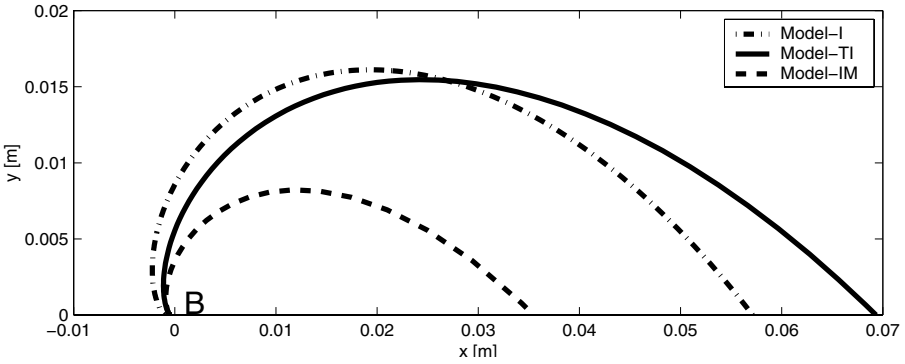

Figure 5: Simulation results with the model-TI, model-I and model-IM for inclined jets ($\theta = 45°$). For given parameters the switching point A does not exist.
.

The corresponding curve to **Model-TI** consists on two parts. First part of the corresponding curve (the solid line between B and A) is obtained by the modified Taylors model (30)-(35). At that part the droplets are not produced. The curve starts at the point B with $r_e(\pi) = 0.5\tilde{R}_{max}(\pi, \theta)$ because of obstacle. If at some ϕ_A the radius $r_e(\phi_A) > 0.99\tilde{R}_{max}(\phi_A, \theta)$, then for the rest the model-IM (37)- (38) is used. At the point A an edge is formed (similar as in Taylors experiments in the case $\theta = 90°$).

In Fig.3 the results for $\theta = 70°$ can be seen. The solid line shows results obtained by the model-TI. For this θ switching point can be very well observed (point A). Both other curves, produced by model-I and model-IM are relatively close to the solid line. But it is necessary to stress that there are large qualitative differences. Model-I and model-IM assume that on the whole boundary of the liquid film droplets are produced. Model-TI proposes that on the first part (the solid line between B and A) no droplets are produced. When we follow Taylors observations, then in the practice both kind of solutions can be noted (sometimes droplets are produced close to the obstacle and sometimes not).

If the angle θ decreases (Fig. 4 corresponds to the angle $\theta = 60°$), then the point A is moving on the right. It means that in some cases on large part of the liquid film no droplets are produced. For given parameters the qualitative and quantitative difference between two possible regimes becomes larger.

If the same model parameters are used as previously but only the angle θ is changed to 45° (Fig. 5), then the model-TI can not fulfill condition $r_e(\phi) > \tilde{R}_{max}(\phi)$ and the point A is not build. It means that droplets can be produced only at the end of film (the polar angle $\phi = 0$). If the models are true, then in this case two very different regimes of the liquid film must be observed (in dependence of wire properties):

- on the whole boundary of the liquid film droplets are produced,
- only on the end of the liquid film droplets are produced.

It is clear that in both cases spectra of generated droplets must be also very different. From this point of view investigation of reasons for two different regimes would be very important for real applications.

5 Conclusions and outlook

Interaction of the liquid film with obstacles can lead to interesting phenomena as already Taylor observed. In dependence of properties of the obstacle droplets can be generated near the contact point or not. In the paper some models for the shape estimation of the liquid film are proposed and corresponding numerical solutions are obtained.

Two types of solution produced by Taylor's model agree qualitatively with Taylor's experiments. If close to obstacle droplets are not generated, then the simulated boundary curve has an edge (point A in Fig. 2). The other type of the solution (cardioid) has a greater curvature. More exact comparison with experiments is not possible because of absence of experimental data.

Numerical experiments with the model for inclined jets show that also for $\theta \neq 90^\circ$ two different types of solution can be obtained. The most interesting is the solution corresponding to the model-TI. In dependence on the angle θ the switching point A can have different positions. If the angle θ decreases, then the part of the film, which does not produce droplets, can increase. There exist also values of parameters at which the point A does not appear (see Fig. 5).

It would be interesting to investigate, how important in the practice is the regime, when on the edge no droplets are produced. The most important question here is, how to manage these regimes. From the Taylors paper [6] it is not possibly clearly to define, under which conditions one or other regime can appear.

References

[1] W.H. Lai W.Huang and T.L.Jiang. Characteristic study on the like-doublet impinging jets atomization. *Atomization and Sprays*, 9:277–289, 1999.

[2] H.M. Ryan W.E. Anderson S. Pal and R.J. Santoro. Atomization characteristics of impinging liquid jets. *Journal of Propulsion and Power*, 11(1):135–145, 1995.

[3] E.A. Ibrahim and A.J. Przekwas. Impinging jets atomization. *Phys. Fluids*, A 3 (12):2981–2987, 1991.

[4] S.G. Taylor. The dynamics of thin sheets of fluid 1. water bells. *Proc. R. Soc. London Ser. A*, 253:289–295, 1959.

[5] S.G. Taylor. The dynamics of thin sheets of fluid 2. waves on fluid sheets. *Proc. R. Soc. London Ser. A*, 253:296–312, 1959.

[6] S.G. Taylor. The dynamics of thin sheets of fluid 3. disintegration of fluid sheets. *Proc. R. Soc. London Ser. A*, 253:313–321, 1959.

[7] S.G. Taylor. Formation of thin flat sheets of water. *Proc. R. Soc. London Ser. A*, 259:1–17, 1960.

[8] N. Dombrowski and W.R. Johns. The aerodynamic instability and disintegration of viscous liquid sheets. *Chemical Engineering Science*, 18:203–214, 1963.

[9] Y.-B. Shen and D. Poulikakos. Thickness variation of a liquid sheet formed by two impinging jets using holographic interferometry. *Transactions of the ASME, Journal of Fluid Engineering*, 120:482–487, 1998.

[10] H.S. Couto and D. Bastos-Netto. Modelling droplet size distribution from impinging jets. *J. of Propulsion and Power*, 7(4):654–656, 1991.

[11] K. Oswatitsch L. Prandtl and K. Wieghardt. *Führer durch die Strömungslehre*. Friedr. Vieweg und Sohn, Braunschweig/Wiesbaden, 1984.

Bisher erschienene Berichte des Fraunhofer ITWM

Die PDF-Files der folgenden Berichte finden Sie unter:
www.itwm.fhg.de/zentral/berichte.html

1. D. Hietel, K. Steiner, J. Struckmeier

A Finite - Volume Particle Method for Compressible Flows

We derive a new class of particle methods for conservation laws, which are based on numerical flux functions to model the interactions between moving particles. The derivation is similar to that of classical Finite-Volume methods; except that the fixed grid structure in the Finite-Volume method is substituted by so-called mass packets of particles. We give some numerical results on a shock wave solution for Burgers equation as well as the well-known one-dimensional shock tube problem.
(19 S., 1998)

2. M. Feldmann, S. Seibold

Damage Diagnosis of Rotors: Application of Hilbert Transform and Multi-Hypothesis Testing

In this paper, a combined approach to damage diagnosis of rotors is proposed. The intention is to employ signal-based as well as model-based procedures for an improved detection of size and location of the damage. In a first step, Hilbert transform signal processing techniques allow for a computation of the signal envelope and the instantaneous frequency, so that various types of non-linearities due to a damage may be identified and classified based on measured response data. In a second step, a multi-hypothesis bank of Kalman Filters is employed for the detection of the size and location of the damage based on the information of the type of damage provided by the results of the Hilbert transform.
Keywords:
Hilbert transform, damage diagnosis, Kalman filtering, non-linear dynamics
(23 S., 1998)

3. Y. Ben-Haim, S. Seibold

Robust Reliability of Diagnostic Multi-Hypothesis Algorithms: Application to Rotating Machinery

Damage diagnosis based on a bank of Kalman filters, each one conditioned on a specific hypothesized system condition, is a well recognized and powerful diagnostic tool. This multi-hypothesis approach can be applied to a wide range of damage conditions. In this paper, we will focus on the diagnosis of cracks in rotating machinery. The question we address is: how to optimize the multi-hypothesis algorithm with respect to the uncertainty of the spatial form and location of cracks and their resulting dynamic effects. First, we formulate a measure of the reliability of the diagnostic algorithm, and then we discuss modifications of the diagnostic algorithm for the maximization of the reliability. The reliability of a diagnostic algorithm is measured by the amount of uncertainty consistent with no-failure of the diagnosis. Uncertainty is quantitatively represented with convex models.
Keywords:
Robust reliability, convex models, Kalman filtering, multi-hypothesis diagnosis, rotating machinery, crack diagnosis
(24 S., 1998)

4. F.-Th. Lentes, N. Siedow

Three-dimensional Radiative Heat Transfer in Glass Cooling Processes

For the numerical simulation of 3D radiative heat transfer in glasses and glass melts, practically applicable mathematical methods are needed to handle such problems optimal using workstation class computers. Since the exact solution would require super-computer capabilities we concentrate on approximate solutions with a high degree of accuracy. The following approaches are studied: 3D diffusion approximations and 3D ray-tracing methods.
(23 S., 1998)

5. A. Klar, R. Wegener

A hierarchy of models for multilane vehicular traffic
Part I: Modeling

In the present paper multilane models for vehicular traffic are considered. A microscopic multilane model based on reaction thresholds is developed. Based on this model an Enskog like kinetic model is developed. In particular, care is taken to incorporate the correlations between the vehicles. From the kinetic model a fluid dynamic model is derived. The macroscopic coefficients are deduced from the underlying kinetic model. Numerical simulations are presented for all three levels of description in [10]. Moreover, a comparison of the results is given there.
(23 S., 1998)

Part II: Numerical and stochastic investigations

In this paper the work presented in [6] is continued. The present paper contains detailed numerical investigations of the models developed there. A numerical method to treat the kinetic equations obtained in [6] are presented and results of the simulations are shown. Moreover, the stochastic correlation model used in [6] is described and investigated in more detail.
(17 S., 1998)

6. A. Klar, N. Siedow

Boundary Layers and Domain Decomposition for Radiative Heat Transfer and Diffusion Equations: Applications to Glass Manufacturing Processes

In this paper domain decomposition methods for radiative transfer problems including conductive heat transfer are treated. The paper focuses on semi-transparent materials, like glass, and the associated conditions at the interface between the materials. Using asymptotic analysis we derive conditions for the coupling of the radiative transfer equations and a diffusion approximation. Several test cases are treated and a problem appearing in glass manufacturing processes is computed. The results clearly show the advantages of a domain decomposition approach. Accuracy equivalent to the solution of the global radiative transfer solution is achieved, whereas computation time is strongly reduced.
(24 S., 1998)

7. I. Choquet

Heterogeneous catalysis modelling and numerical simulation in rarified gas flows Part I: Coverage locally at equilibrium

A new approach is proposed to model and simulate numerically heterogeneous catalysis in rarefied gas flows. It is developed to satisfy all together the following points:
1) describe the gas phase at the microscopic scale, as required in rarefied flows,
2) describe the wall at the macroscopic scale, to avoid prohibitive computational costs and consider not only crystalline but also amorphous surfaces,
3) reproduce on average macroscopic laws correlated with experimental results and
4) derive analytic models in a systematic and exact way.
The problem is stated in the general framework of a non static flow in the vicinity of a catalytic and non porous surface (without aging). It is shown that the exact and systematic resolution method based on the Laplace transform, introduced previously by the author to model collisions in the gas phase, can be extended to the present problem. The proposed approach is applied to the modelling of the Eley-Rideal and Langmuir-Hinshelwood recombinations, assuming that the coverage is locally at equilibrium. The models are developed considering one atomic species and extended to the general case of several atomic species. Numerical calculations show that the models derived in this way reproduce with accuracy behaviors observed experimentally.
(24 S., 1998)

8. J. Ohser, B. Steinbach, C. Lang

Efficient Texture Analysis of Binary Images

A new method of determining some characteristics of binary images is proposed based on a special linear filtering. This technique enables the estimation of the area fraction, the specific line length, and the specific integral of curvature. Furthermore, the specific length of the total projection is obtained, which gives detailed information about the texture of the image. The influence of lateral and directional resolution depending on the size of the applied filter mask is discussed in detail. The technique includes a method of increasing directional resolution for texture analysis while keeping lateral resolution as high as possible.
(17 S., 1998)

9. J. Orlik

Homogenization for viscoelasticity of the integral type with aging and shrinkage

A multi-phase composite with periodic distributed inclusions with a smooth boundary is considered in this contribution. The composite component materials are supposed to be linear viscoelastic and aging (of the non-convolution integral type, for which the Laplace transform with respect to time is not effectively applicable) and are subjected to isotropic shrinkage. The free shrinkage deformation can be considered as a fictitious temperature deformation in the behavior law. The procedure presented in this paper proposes a way to determine average (effective homogenized) viscoelastic and shrinkage (temperature) composite properties and the homogenized stress-field from known properties of the

components. This is done by the extension of the asymptotic homogenization technique known for pure elastic non-homogeneous bodies to the non-homogeneous thermo-viscoelasticity of the integral non-convolution type. Up to now, the homogenization theory has not covered viscoelasticity of the integral type.
Sanchez-Palencia (1980), Francfort & Suquet (1987) (see [2], [9]) have considered homogenization for viscoelasticity of the differential form and only up to the first derivative order. The integral-modeled viscoelasticity is more general then the differential one and includes almost all known differential models. The homogenization procedure is based on the construction of an asymptotic solution with respect to a period of the composite structure. This reduces the original problem to some auxiliary boundary value problems of elasticity and viscoelasticity on the unit periodic cell, of the same type as the original non-homogeneous problem. The existence and uniqueness results for such problems were obtained for kernels satisfying some constrain conditions. This is done by the extension of the Volterra integral operator theory to the Volterra operators with respect to the time, whose 1 kernels are space linear operators for any fixed time variables. Some ideas of such approach were proposed in [11] and [12], where the Volterra operators with kernels depending additionally on parameter were considered. This manuscript delivers results of the same nature for the case of the space-operator kernels.
(20 S., 1998)

10. J. Mohring

Helmholtz Resonators with Large Aperture

The lowest resonant frequency of a cavity resonator is usually approximated by the classical Helmholtz formula. However, if the opening is rather large and the front wall is narrow this formula is no longer valid. Here we present a correction which is of third order in the ratio of the diameters of aperture and cavity. In addition to the high accuracy it allows to estimate the damping due to radiation. The result is found by applying the method of matched asymptotic expansions. The correction contains form factors describing the shapes of opening and cavity. They are computed for a number of standard geometries. Results are compared with numerical computations.
(21 S., 1998)

11. H. W. Hamacher, A. Schöbel

On Center Cycles in Grid Graphs

Finding "good" cycles in graphs is a problem of great interest in graph theory as well as in locational analysis. We show that the center and median problems are NP hard in general graphs. This result holds both for the variable cardinality case (i.e. all cycles of the graph are considered) and the fixed cardinality case (i.e. only cycles with a given cardinality p are feasible). Hence it is of interest to investigate special cases where the problem is solvable in polynomial time.
In grid graphs, the variable cardinality case is, for instance, trivially solvable if the shape of the cycle can be chosen freely.
If the shape is fixed to be a rectangle one can analyze rectangles in grid graphs with, in sequence, fixed dimension, fixed cardinality, and variable cardinality. In all cases a complete characterization of the optimal cycles and closed form expressions of the optimal objective values are given, yielding polynomial time algorithms for all cases of center rectangle problems.
Finally, it is shown that center cycles can be chosen as rectangles for small cardinalities such that the center cycle problem in grid graphs is in these cases completely solved.
(15 S., 1998)

12. H. W. Hamacher, K.-H. Küfer

Inverse radiation therapy planning - a multiple objective optimisation approach

For some decades radiation therapy has been proved successful in cancer treatment. It is the major task of clinical radiation treatment planning to realize on the one hand a high level dose of radiation in the cancer tissue in order to obtain maximum tumor control. On the other hand it is obvious that it is absolutely necessary to keep in the tissue outside the tumor, particularly in organs at risk, the unavoidable radiation as low as possible.
No doubt, these two objectives of treatment planning - high level dose in the tumor, low radiation outside the tumor - have a basically contradictory nature. Therefore, it is no surprise that inverse mathematical models with dose distribution bounds tend to be infeasible in most cases. Thus, there is need for approximations compromising between overdosing the organs at risk and underdosing the target volume.
Differing from the currently used time consuming iterative approach, which measures deviation from an ideal (non-achievable) treatment plan using recursively trial-and-error weights for the organs of interest, we go a new way trying to avoid a priori weight choices and consider the treatment planning problem as a multiple objective linear programming problem: with each organ of interest, target tissue as well as organs at risk, we associate an objective function measuring the maximal deviation from the prescribed doses.
We build up a data base of relatively few efficient solutions representing and approximating the variety of Pareto solutions of the multiple objective linear programming problem. This data base can be easily scanned by physicians looking for an adequate treatment plan with the aid of an appropriate online tool.
(14 S., 1999)

13. C. Lang, J. Ohser, R. Hilfer

On the Analysis of Spatial Binary Images

This paper deals with the characterization of microscopically heterogeneous, but macroscopically homogeneous spatial structures. A new method is presented which is strictly based on integral-geometric formulae such as Crofton's intersection formulae and Hadwiger's recursive definition of the Euler number. The corresponding algorithms have clear advantages over other techniques. As an example of application we consider the analysis of spatial digital images produced by means of Computer Assisted Tomography.
(20 S., 1999)

14. M. Junk

On the Construction of Discrete Equilibrium Distributions for Kinetic Schemes

A general approach to the construction of discrete equilibrium distributions is presented. Such distribution functions can be used to set up Kinetic Schemes as well as Lattice Boltzmann methods. The general principles are also applied to the construction of Chapman Enskog distributions which are used in Kinetic Schemes for compressible Navier-Stokes equations.
(24 S., 1999)

15. M. Junk, S. V. Raghurame Rao

A new discrete velocity method for Navier-Stokes equations

The relation between the Lattice Boltzmann Method, which has recently become popular, and the Kinetic Schemes, which are routinely used in Computational Fluid Dynamics, is explored. A new discrete velocity model for the numerical solution of Navier-Stokes equations for incompressible fluid flow is presented by combining both the approaches. The new scheme can be interpreted as a pseudo-compressibility method and, for a particular choice of parameters, this interpretation carries over to the Lattice Boltzmann Method.
(20 S., 1999)

16. H. Neunzert

Mathematics as a Key to Key Technologies

The main part of this paper will consist of examples, how mathematics really helps to solve industrial problems; these examples are taken from our Institute for Industrial Mathematics, from research in the Technomathematics group at my university, but also from ECMI groups and a company called TecMath, which originated 10 years ago from my university group and has already a very successful history.
(39 S. (vier PDF-Files), 1999)

17. J. Ohser, K. Sandau

Considerations about the Estimation of the Size Distribution in Wicksell's Corpuscle Problem

Wicksell's corpuscle problem deals with the estimation of the size distribution of a population of particles, all having the same shape, using a lower dimensional sampling probe. This problem was originary formulated for particle systems occurring in life sciences but its solution is of actual and increasing interest in materials science. From a mathematical point of view, Wicksell's problem is an inverse problem where the interesting size distribution is the unknown part of a Volterra equation. The problem is often regarded ill-posed, because the structure of the integrand implies unstable numerical solutions. The accuracy of the numerical solutions is considered here using the condition number, which allows to compare different numerical methods with different (equidistant) class sizes and which indicates, as one result, that a finite section thickness of the probe reduces the numerical problems. Furthermore, the relative error of estimation is computed which can be split into two parts. One part consists of the relative discretization error that increases for increasing class size, and the second part is related to the relative statistical error which increases with decreasing class size. For both parts, upper bounds can be given and the sum of them indicates an optimal class width depending on some specific constants.
(18 S., 1999)

18. E. Carrizosa, H. W. Hamacher, R. Klein, S. Nickel

Solving nonconvex planar location problems by finite dominating sets

It is well-known that some of the classical location problems with polyhedral gauges can be solved in polynomial time by finding a finite dominating set, i. e. a finite set of candidates guaranteed to contain at least one optimal location.
In this paper it is first established that this result holds for a much larger class of problems than currently considered in the literature. The model for which this result can be proven includes, for instance, location problems with attraction and repulsion, and location-allocation problems. Next, it is shown that the approximation of general gauges by polyhedral ones in the objective function of our general model can be analyzed with regard to the subsequent error in the optimal objective value. For the approximation problem two different approaches are described, the sandwich procedure and the greedy algorithm. Both of these approaches lead - for fixed epsilon - to polynomial approximation algorithms with accuracy epsilon for solving the general model considered in this paper.
Keywords:
Continuous Location, Polyhedral Gauges, Finite Dominating Sets, Approximation, Sandwich Algorithm, Greedy Algorithm
(19 S., 2000)

19. A. Becker

A Review on Image Distortion Measures

Within this paper we review image distortion measures. A distortion measure is a criterion that assigns a "quality number" to an image. We distinguish between mathematical distortion measures and those distortion measures in-cooperating a priori knowledge about the imaging devices (e. g. satellite images), image processing algorithms or the human physiology. We will consider representative examples of different kinds of distortion measures and are going to discuss them.
Keywords:
Distortion measure, human visual system
(26 S., 2000)

20. H. W. Hamacher, M. Labbé, S. Nickel, T. Sonneborn

Polyhedral Properties of the Uncapacit*ated Multiple Allocation Hub Location Problem*

We examine the feasibility polyhedron of the uncapacitated hub location problem (UHL) with multiple allocation, which has applications in the fields of air passenger and cargo transportation, telecommunication and postal delivery services. In particular we determine the dimension and derive some classes of facets of this polyhedron. We develop some general rules about lifting facets from the uncapacitated facility location (UFL) for UHL and projecting facets from UHL to UFL. By applying these rules we get a new class of facets for UHL which dominates the inequalities in the original formulation. Thus we get a new formulation of UHL whose constraints are all facet–defining. We show its superior computational performance by benchmarking it on a well known data set.
Keywords:
integer programming, hub location, facility location, valid inequalities, facets, branch and cut
(21 S., 2000)

21. H. W. Hamacher, A. Schöbel

Design of Zone Tariff Systems in Public Transportation

Given a public transportation system represented by its stops and direct connections between stops, we consider two problems dealing with the prices for the customers: The fare problem in which subsets of stops are already aggregated to zones and "good" tariffs have to be found in the existing zone system. Closed form solutions for the fare problem are presented for three objective functions. In the zone problem the design of the zones is part of the problem. This problem is NP hard and we therefore propose three heuristics which prove to be very successful in the redesign of one of Germany's transportation systems.
(30 S., 2001)

22. D. Hietel, M. Junk, R. Keck, D. Teleaga:

The Finite-Volume-Particle Method for Conservation Laws

In the Finite-Volume-Particle Method (FVPM), the weak formulation of a hyperbolic conservation law is discretized by restricting it to a discrete set of test functions. In contrast to the usual Finite-Volume approach, the test functions are not taken as characteristic functions of the control volumes in a spatial grid, but are chosen from a partition of unity with smooth and overlapping partition functions (the particles), which can even move along prescribed velocity fields. The information exchange between particles is based on standard numerical flux functions. Geometrical information, similar to the surface area of the cell faces in the Finite-Volume Method and the corresponding normal directions are given as integral quantities of the partition functions.
After a brief derivation of the Finite-Volume-Particle Method, this work focuses on the role of the geometric coefficients in the scheme.
(16 S., 2001)

23. T. Bender, H. Hennes, J. Kalcsics, M. T. Melo, S. Nickel

Location Software and Interface with GIS and Supply Chain Management

The objective of this paper is to bridge the gap between location theory and practice. To meet this objective focus is given to the development of software capable of addressing the different needs of a wide group of users. There is a very active community on location theory encompassing many research fields such as operations research, computer science, mathematics, engineering, geography, economics and marketing. As a result, people working on facility location problems have a very diverse background and also different needs regarding the software to solve these problems. For those interested in non-commercial applications (e. g. students and researchers), the library of location algorithms (LoLA can be of considerable assistance. LoLA contains a collection of efficient algorithms for solving planar, network and discrete facility location problems. In this paper, a detailed description of the functionality of LoLA is presented. In the fields of geography and marketing, for instance, solving facility location problems requires using large amounts of demographic data. Hence, members of these groups (e. g. urban planners and sales managers) often work with geographical information too s. To address the specific needs of these users, LoLA was inked to a geographical information system (GIS) and the details of the combined functionality are described in the paper. Finally, there is a wide group of practitioners who need to solve large problems and require special purpose software with a good data interface. Many of such users can be found, for example, in the area of supply chain management (SCM). Logistics activities involved in strategic SCM include, among others, facility location planning. In this paper, the development of a commercial location software tool is also described. The too is embedded in the Advanced Planner and Optimizer SCM software developed by SAP AG, Walldorf, Germany. The paper ends with some conclusions and an outlook to future activities.
Keywords:
facility location, software development, geographical information systems, supply chain management.
(48 S., 2001)

24. H. W. Hamacher, S. A. Tjandra

Mathematical Modelling of Evacuation Problems: A State of Art

This paper details models and algorithms which can be applied to evacuation problems. While it concentrates on building evacuation many of the results are applicable also to regional evacuation. All models consider the time as main parameter, where the travel time between components of the building is part of the input and the overall evacuation time is the output. The paper distinguishes between macroscopic and microscopic evacuation models both of which are able to capture the evacuees' movement over time.
Macroscopic models are mainly used to produce good lower bounds for the evacuation time and do not consider any individual behavior during the emergency situation. These bounds can be used to analyze existing buildings or help in the design phase of planning a building. Macroscopic approaches which are based on dynamic network flow models (minimum cost dynamic flow, maximum dynamic flow, universal maximum flow, quickest path and quickest flow) are described. A special feature of the presented approach is the fact, that travel times of evacuees are not restricted to be constant, but may be density dependent. Using multicriteria optimization priority regions and blockage due to fire or smoke may be considered. It is shown how the modelling can be done using time parameter either as discrete or continuous parameter.
Microscopic models are able to model the individual evacuee's characteristics and the interaction among evacuees which influence their movement. Due to the corresponding huge amount of data one uses simulation approaches. Some probabilistic laws for individual evacuee's movement are presented. Moreover ideas to model the evacuee's movement using cellular automata (CA) and resulting software are presented.
In this paper we will focus on macroscopic models and only summarize some of the results of the microscopic approach. While most of the results are applicable to general evacuation situations, we concentrate on building evacuation.
(44 S., 2001)

25. J. Kuhnert, S. Tiwari

Grid free method for solving the Poisson equation

A Grid free method for solving the Poisson equation is presented. This is an iterative method. The method is based on the weighted least squares approximation in which the Poisson equation is enforced to be satisfied in every iterations. The boundary conditions can also be enforced in the iteration process. This is a local approximation procedure. The Dirichlet, Neumann and mixed boundary value problems on a unit square are presented and the analytical solutions are compared with the exact solutions. Both solutions matched perfectly.
Keywords:
Poisson equation, Least squares method, Grid free method
(19 S., 2001)

26. T. Götz, H. Rave, D. Reinel-Bitzer, K. Steiner, H. Tiemeier

Simulation of the fiber spinning process

To simulate the influence of process parameters to the melt spinning process a fiber model is used and coupled with CFD calculations of the quench air flow. In the fiber model energy, momentum and mass balance are solved for the polymer mass flow. To calculate the quench air the Lattice Boltzmann method is used. Simulations and experiments for different process parameters and hole configurations are compared and show a good agreement.
Keywords:
Melt spinning, fiber model, Lattice Boltzmann, CFD
(19 S., 2001)

27. A. Zemitis

On interaction of a liquid film with an obstacle

In this paper mathematical models for liquid films generated by impinging jets are discussed. Attention is stressed to the interaction of the liquid film with some obstacle. S. G. Taylor [Proc. R. Soc. London Ser. A 253, 313 (1959)] found that the liquid film generated by impinging jets is very sensitive to properties of the wire which was used as an obstacle. The aim of this presentation is to propose a modification of the Taylor's model, which allows to simulate the film shape in cases, when the angle between jets is different from 180°. Numerical results obtained by discussed models give two different shapes of the liquid film similar as in Taylors experiments. These two shapes depend on the regime: either droplets are produced close to the obstacle or not. The difference between two regimes becomes larger if the angle between jets decreases. Existence of such two regimes can be very essential for some applications of impinging jets, if the generated liquid film can have a contact with obstacles.
Keywords:
impinging jets, liquid film, models, numerical solution, shape
(22 S., 2001)

28. I. Ginzburg, K. Steiner

Free surface lattice-Boltzmann method to model the filling of expanding cavities by Bingham Fluids

The filling process of viscoplastic metal alloys and plastics in expanding cavities is modelled using the lattice Boltzmann method in two and three dimensions. These models combine the regularized Bingham model for viscoplastic with a free-interface algorithm. The latter is based on a modified immiscible lattice Boltzmann model in which one species is the fluid and the other one is considered as vacuum. The boundary conditions at the curved liquid-vacuum interface are met without any geometrical front reconstruction from a first-order Chapman-Enskog expansion. The numerical results obtained with these models are found in good agreement with available theoretical and numerical analysis.
Keywords:
Generalized LBE, free-surface phenomena, interface boundary conditions, filling processes, Bingham viscoplastic model, regularized models
(22 S., 2001)